

Polymeric forms of carbon in dense lithium carbide

Xing-Qiu Chen,^{1,*} C. L. Fu,¹ C. Franchini²

¹ Oak Ridge National Laboratory, Materials Science and Technology Division, Oak Ridge, TN, 37831, USA

² Faculty of Physics, University of Vienna and Center for Computational Materials Science, A-1090 Vienna, Austria

* Current address: Shenyang National Laboratory for Materials Sciences, Institute for Metal Research, Chinese Academy of Sciences, Shenyang, 110016, P. R. China

E-mail: corresponding author: xingqiu.chen@imr.ac.cn

Abstract. The immense interest in carbon nanomaterials continues to stimulate intense research activities aimed to realize carbon nanowires, since linear chains of carbon atoms are expected to display novel and technologically relevant optical, electrical and mechanical properties. Although various allotropes of carbon (e.g., diamond, nanotubes, graphene, etc.) are among the best known materials, it remains challenging to stabilize carbon in the one-dimensional form because of the difficulty to suitably saturate the dangling bonds of carbon. Here, we show through first-principles calculations that ordered polymeric carbon chains can be stabilized in solid Li_2C_2 under moderate pressure. This pressure-induced phase (above 5 GPa) consists of parallel arrays of twofold zigzag carbon chains embedded in lithium cages, which display a metallic character due to the formation of partially occupied carbon lone-pair states in sp^2 -like hybrids. It is found that this phase remains the most favorable one in a wide range of pressure. At extreme pressure (larger than 215 GPa) a structural and electronic phase transition towards an insulating single-bonded threefold-coordinated carbon network is predicted.

Atomic carbon is stabilized in innumerable molecular configurations (allotropes) characterized by different combinations of sp^3 , sp^2 and sp hybrid orbitals[1]. The most well-known allotropes of carbon are diamond with its sp^3 bonds, graphite, graphene, fullerene and nanotubes with sp^2 hybrids, as well as transitional forms of carbon with mixed hybridizations such as amorphous carbon. The properties of carbon nanomaterials are the subject of an intensive research activity, motivated by several reasons ranging from their potentially revolutionary technological applications to more fundamental issues such as the understanding of interstellar clouds and C-based superconductivity. In this context, linear carbon chains have gained a renewed attention in recent years since they are considered precursors in the formation of carbon nanomaterials. However, despite the intensive experimental effort, the synthesis of ideal solid carbon constituted by linear chains of carbon (polyynes or cumulenes) is still a major challenge[2, 3, 4]. According to the most recent literature, three different processes can lead to the synthesis of atomic wires of carbon: (i) by removing carbon atoms from graphene using energetic electron irradiation[5], (ii) by assembling

carbon cluster on graphitic nanofragments[6] and (iii) by chemical, electrochemical, and other sophisticated techniques as discussed in a recent review[7]. Within a simplified view, all linear conjugated polymers with a chain-like structure may be considered as one-dimensional (1D) carbon phases in which dangling bonds of carbon are suitably saturated. This is the case, for example, for polyacetylene $(C_2H_2)_n$, where each carbon is covalently bonded to one hydrogen and is connected to the two neighboring carbon atoms by alternating single and double bonds [8]. The alternation of bonds and the resulting insulating groundstate is induced by a Peierls-like instability. Massive doping, however, lifts the Peierls instability and leads to a highly conducting metallic regime[9, 10].

Like hydrogen, lithium forms several binary compounds with carbon,[11] but none of them reveal 1D features similar to $(C_2H_2)_n$. On the carbon-rich side the best-known materials are lithium-graphite intercalation compounds such as LiC_6 [12], whereas on the Li-rich side the only compound which can be produced directly from the elements is Li_2C_2 , characterized by triple bonded $C\equiv C$ dimers.[13, 14] Considering that charge is donated from Li to C in Li_2C_2 , one might expect that Li_2C_2 under pressure could be transformed to a polyacetylene-like structure with 1D characteristics. This expectation is based on two reasons: (1) the pressure decreases the lattice spacing and, therefore, increases the interaction between $C\equiv C$ dimers, and (2) the role of the C-H bond in C_2H_2 could be replaced by that of the lone-pair orbital in Li_2C_2 in the stabilization of a chain-like structure.

In this study, we applied density functional theory (DFT) to perform an extensive search for possible structural candidates for Li_2C_2 under pressure. Over more than 200 crystal structures were explored with different local environment of carbon atoms. We find that by application of low pressure (5 GPa) triple bonded $C\equiv C$ dimers in Li_2C_2 can be transformed into metallic carbon linear chains encapsulated in lithium cages. The pressure-dependent evolution of this structure show that the carbon chains are stable over a wide range of compressions, and are eventually converted into insulating single-bonded C-C cubic networks above 215 GPa. Thus, our computational experiment reveals that it is possible to construct conductive linear-chains of carbon by simply compressing solid Li_2C_2 at pressures accessible to modern high-pressure technology. Considering that Li_2C_2 can be easily produced and that, unlike polyacetylene, the conductivity arises naturally upon pressure without the need of any doping treatment, we believe that our study will stimulate prompt experimental investigations in the foreseeable future.

First-principles calculations were mainly performed using the Vienna *ab initio* Simulation Package (VASP) [23] with the ion-electron interaction described by the projector augmented wave potential (PAW) [25]. We used the generalized gradient approximation within the Perdew-Burke-Ernzerhof (PBE) parameterization scheme [26] for the exchange-correlation functional. Brillouin-zone integrations were performed for special k points according to Monkhorst and Pack technique. The energy cutoff for the plane-wave expansion of eigenfunctions was set to 500 eV. Optimization of structural parameters was achieved by the minimization of forces and stress tensors. Highly

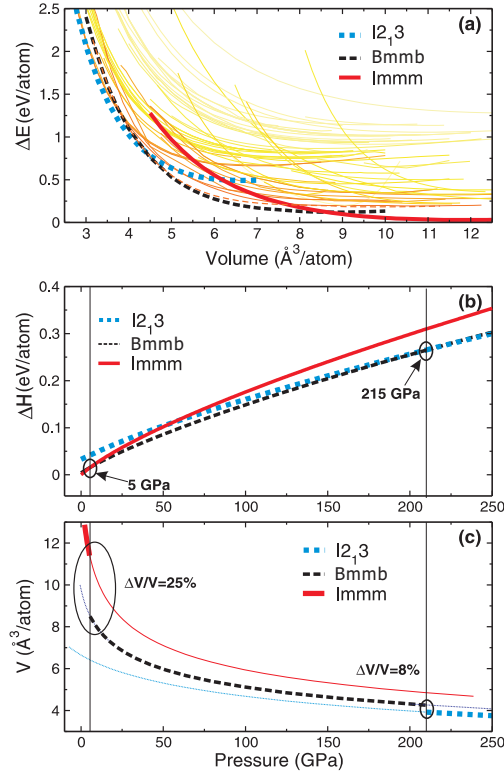


Figure 1. DFT calculated energy/pressure relations for Li_2C_2 . (a): energy difference (ΔE) vs. volume (V), (b): enthalpy difference (ΔH) vs. pressure, and (c): volume (V) vs. pressure. In panels (a) and (b), the energy zero refers to the energy of the *Immm* phase at 0 GPa. The thin curves in panel (a) represent the relationship between ΔE and V for other structures considered here. The thick and thin curves in panel (c) denote the stable and unstable pressure regions for corresponding phases, respectively.

converged results were obtained adopting a very high energy cutoff of 500 eV for the basis sets, and utilizing a dense $12 \times 12 \times 12$ \vec{k} -point grid for the Brillouin zone integration. For the proposed Bmmb phase, phonon spectra under pressures have been performed using density functional perturbation theory as implemented in the Quantum-ESPRESSO code [27], using norm-conserving pseudopotentials.

Structural properties: the prediction of crystal structure by means of first-principles methods remains a complex task and a good choice of initial configurations is crucial to perform an accurate structural search. Recent studies have demonstrated that a large pool of randomly selected initial configurations is a necessary ingredient for an accurate structural search [28, 29, 30]. In our study, to form random unit cells we have chosen Bravais matrix with random lattice parameters and random cell angles (including all seven crystal classes). For each initial configuration the internal degrees of freedom (atomic positions) were selected by a random modification of several structural possibilities found in literature. Finally, the unit cell volume was properly scaled in order to reproduce the desired pressure. At this point we have performed a full structural optimization (cell shape, lattice parameters and internal positions) for each starting configuration according to a quasi-Newton algorithm where forces and the

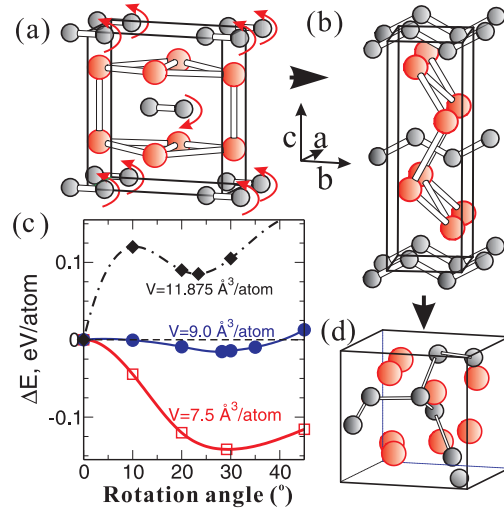


Figure 2. Schematic illustration of the pressure-induced structural sequence (a) Immm \rightarrow (b) Bmmb \rightarrow (d) I2₁3 with smaller balls for C and larger balls for Li. Curved arrows in panel (a) indicate the rotation of C \equiv C pairs which leads to the zigzag C-C arrangement sketched in panel (b). Panel (d) illustrates the threefold carbon polymeric network. Panel (c) shows the change in energy (ΔE) when rotating the C \equiv C pairs as shown in panel (a) for three different volumes of the Immm structure. Note that the lattice parameters are allowed to relax (but with the constraint of constant volume) in obtaining each of the curves in (c).

stress tensor are used to determine the search directions for finding the equilibrium configuration. This computational procedure reduces substantially the risk of being trapped in metastable solution (local minima of the potential energy surface) and permits the exploration of a large number of different structures. We have tested local carbon environments including triple bonded dimers, carbon linear chains (polyyne- and polyacetylene- like structures) and three-connected nets[31] [planar (graphite like), puckered (α -arsenic structure) or more complex conformations such as those observed in ThSi₂[32], SrSi₂[33] and DyGe₃[34].

The energy/pressure relations derived from our DFT structural search are depicted in Fig. 1. The low-pressure insulating orthorhombic Immm phase [Fig. 2(a)] is correctly predicted to be the lowest-energy phase at zero pressure, with structural parameters in excellent agreement with experiment (see Table 1). At 5 GPa this phase is transformed into a metallic phase with Bmmb symmetry characterized by zigzag chains of carbon atoms which are embedded in hexagonal Li cages [Fig. 2(b)]. The Bmmb phase remains the most favourable solution until 215 GPa, at which pressure an insulating phase of cubic I2₁3 symmetry with the threefold carbon polymeric network [Fig. 2(c)] is stabilized. The pressure-induced structural evolution is accompanied by a peculiar modulation of the carbon bonds from C \equiv C triply bonded dimers (Immm) to sp^2 -like twofold-coordinated carbon chains (Bmmb), and finally to a sp^3 -like threefold-coordinated carbon network, which is very similar to that in the high-pressure cubic gauche structure of solid nitrogen (cg-N) [15].

Table 1. DFT optimized structural parameters for the Immm (No. 71), Bmmb (No. 63) and I213 (No. 199) structures of Li_2C_2 . Lattice parameters (a , b , and c) and bond length of carbon ($L_{\text{C-C}}$) are given in Å.

Parameters	Expt [14]	DFT (0 GPa)	DFT (5GPa)	DFT (215 GPa)
a	3.652	3.635	3.134	4.172
b	4.831	4.849	2.503	
c	5.434	5.389	7.237	
$L_{\text{C-C}}$	1.226	1.221	1.431	1.597
Li	4j:(0,0.5,0.236)	4j:(0,0.5,0.239)	4c:(0,0.25,0.153)	8a:(0.306, 0.306, 0.306)
C	4g:(0,0.127,0)	4g:(0,0.126, 0)	4c:(0,0.25,0.452)	8a:(0.073, 0.073, 0.073)

At 5 GPa, we find a sudden volume collapse of 25%, as shown in Figure 1(c), related to the Immm \rightarrow Bmmb phase transformation. The Bmmb phase is found to be energetically stable against a phase separation into bcc Li and LiC_6 , as well as against a decomposition into bcc Li and graphite. Here, we should mention that the *ab initio* treatment of graphite within a conventional GGA approach suffers from the well-known limitations related to the fact that van Der Waals (vdW) interactions between graphic layers are poorly described. In order to minimize the effects of vdW errors we have followed the procedure tested by N. Mounet and N. Marzari[16] which consists in the calculation of the equation of state (EOS) in the variable c/a_0 with the in-plane lattice parameter a_0 kept fixed to the experimental value. The so obtained EOS and bulk modulus are in fair agreement with the experimental values[17, 18] and the expected error associated with the GGA binding energy, ~ 0.05 eV/C, does not affect the alloy stability reported here. Additional support for the stability of the proposed Bmmb structure is provided by the absence on any imaginary frequency in the calculated pressure-dependent phonon spectrum reported in Fig. 3.

The predicted pressure-induced structural evolution from the Immm phase to the Bmmb structure can be ascribed to the modification of the lattice parameters (elongation of c and compression of the ab plane of the Immm phase) and concomitant rotations of the carbon dimers, according to Fig. 2(a) and (b). Energetically, the crucial mechanism governing the Immm to Bmmb transition is the rotation of the carbon dimers, as illustrated in Fig. 2 (c). At zero pressure (corresponding to a volume of $V=11.875 \text{ \AA}^3$) the rotation of dimers is highly unfavorable, but with increasing pressure the energy barrier is reduced and disappears at a volume of $V=9.0 \text{ \AA}^3$, corresponding to 5 GPa. Upon this structural transformation, the $\text{C}\equiv\text{C}$ dimers are converted into zigzag carbon chains with a C-C bond length of 1.43 Å and a large inter-chain distance of 3.13 Å. The carbon chains in the Bmmb phase are parallel arrays of polymeric chains along the b axis direction [Fig. 2(b)]. Although the Bmmb phase is calculated to be the most stable in a very wide pressure range of 5 to 215 GPa, at pressures above 150 GPa it becomes very close in energy to a tetragonal phase of $I4_1/amd$ symmetry. In this $I4_1/amd$ phase the carbon atoms also form zigzag chains, but with blocks of chains oriented 90° with

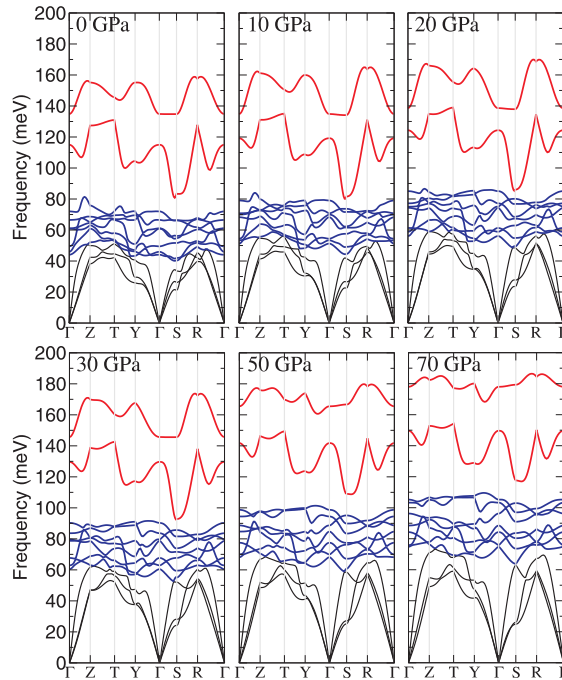


Figure 3. Pressure-dependent phonon dispersions for the proposed Bmmb phase at the pressures of 0, 10, 20, 30, 50, and 70 GPa.

respect to each other, similar to the Ge-network of BaGe_2 [19]. At 215 GPa we predict a second structural transition towards an insulating cubic $\text{I}2_13$ phase [see Fig. 2(d)], accompanied by a volume collapse of 8%. This phase has a σ -character single-bonded C-C bond length of 1.60 Å at 215 GPa, which resembles that of diamond at 0 GPa (1.55 Å). This phase is similar to the high-pressure cubic gauche structure of solid nitrogen (cg-N [20]) as experimentally synthesized by Eremets *et. al.*, [21] and as theoretically studied by us[15].

Electronic properties: at zero pressure the Immm phase exhibits a wide gap of 3.9 eV which slightly decreases upon pressure, reaching the value of 3.7 eV at the critical pressure of 5 GPa, at which the transition towards the metallic Bmmb structure occurs. Upon further compression, the metallic regime is finally destroyed at 215 GPa, at which pressure the most stable $\text{I}2_13$ phase shows a gap of 2.7 eV. The calculated DFT gaps of insulators are generally too small. By performing a screened exchange hybrid density functional calculation for Li_2C_2 within the Heyd-Scuseria-Ernzerhof scheme we obtain a significantly larger gap (5.8 eV) for the Immm phase at 0 GPa.

The bonding property of the metallic Bmmb structure is dominated by sp^2 -like hybrids. Two of the carbon electrons form covalent σ -type bonds [bands b1 and b2 in Fig. 4(a)] connecting neighboring carbons along the zigzag backbone with an bond angle of 123° . These σ -character states [Fig. 4(b)] display quasi-1D features as reflected by a square root singularities [10] in the density of states profile [Fig. 5]. Our analysis also revealed lone-pair orbitals localized at the carbon sites, as depicted in Fig. 4(c). The bands formed by the lone-pair orbitals, however, are overlapped in energy with

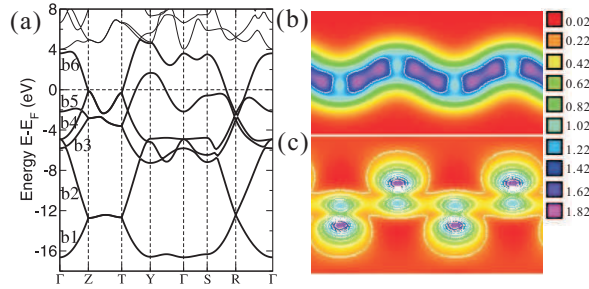


Figure 4. Panel (a): DFT band structures of the Bmmb phases; band labeling, see text. Charge density contours of (b) C-C σ bonded states of bands b1, b2 and (c) lone-pair states of bands b3, b5.

the bands formed by the π -type bonding and antibonding orbitals of carbon. In order to accommodate ten electrons per Li_2C_2 formula unit (with the charge donated from Li to C) in the energy bands of Li_2C_2 , the Fermi level has to intersect both the lone-pair and π -state bands. In other words, there are holes in the lone-pair state and electrons in the antibonding π -state. The electron-deficient lone-pairs are distributed into the fully occupied band b3 and partially filled band b5. Formally, a lone-pair state should trap two electrons but we find that about 1.7e are trapped in band 5. The remaining electrons occupy the π -states, which are characterized by the charge-density lobes aligned perpendicular to the plane defined by the zigzag chains. These orbitals form bands with π -type bonding and antibonding character, as indicated by the respective bands b4 and b6 in Fig. 4(a). The bonding b4 band is fully occupied whereas the antibonding b6 band is partially filled with occupancy of 0.3e.

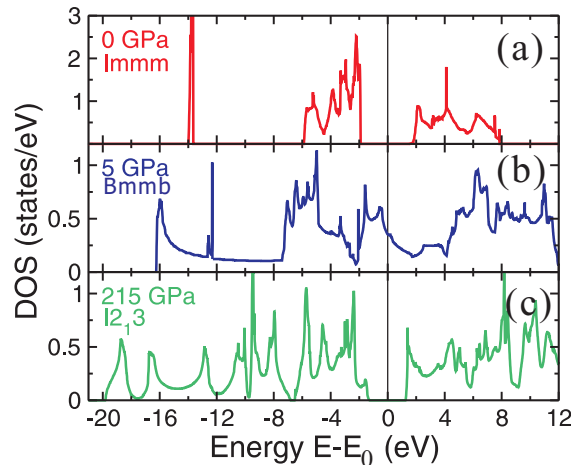


Figure 5. Calculated density of states (DOS) for the Immm (0 GPa), Bmmb (5 GPa), and $I2,3$ (215 GPa) structures. For the Immm and $I2,3$ phases, the energy zero is set in the middle of the gap; For the Bmmb phase, the energy zero is set at the Fermi level.

As mentioned already, conjugate polymers represent the only known producible form of carbon-chains based structures. In order to highlight the structural similarities

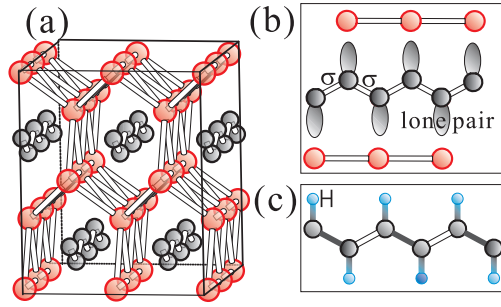


Figure 6. Panel (a): Supercell of the Bmmb structure corresponding to panel (b) of Fig. 2 with small balls for C and large balls for Li. Panel (b): view of a σ bonded C-C chain (bond length 1.45 Å) in which each C atom carries a lone-pair (the more delocalized π bonds are not shown here). Panel (c): similar view of polyacetylene C_2H_2 [8], in which each C atom is connected by a double-bond (length 1.36 Å) and a single-bond (length 1.44 Å) to the neighboring C-atoms. The C-H covalent bond length is 1.02 Å.

between archetypal linear carbon chains of polyacetylene and C-C chains of the Bmmb structure, we compare their corresponding local structure in Fig. 6. In spite of some visual similarity, significant differences can be realized, which explain the distinctly different electronic character: the covalent nature of the C-H bond in polyacetylene is replaced by the ionic C-Li bond in Li_2C_2 , which is stabilized by the formation of the lone-pair in sp^2 -like hybrids. In polyacetylene a Peierls distortion is observed [8] which induces alternating single and double bonds with an angle of 120° and a gap opens up, and substantial doping is required in order to lift the system towards a conducting regime. A different stabilization mechanism is found for the Bmmb phase of Li_2C_2 : holes are created in the lone-pair band b5 which prevents the Peierls-like splitting of states, and thereby the system is metallic.

To ascertain the distinct structural and electronic properties of the predicted Bmmb phase, we have carried out additional calculations with four different supercells containing a larger number of atoms ($Li_{16}C_{16} - 2a \times 2b \times c$, $Li_{24}C_{24} - 2a \times 3b \times c$, $Li_{32}C_{32} - 2a \times 2b \times 2c$, and $Li_{64}C_{64} - 2a \times 4b \times 2c$) and performing the full structural relaxation without any symmetry constrains. Indeed, all derived optimized structures converge to the same Bmmb phase and display identical structural (carbon linear chains) and electronic (metallic sp^2 -like hybrids) characteristics. This computational experiment unambiguously prove that the linear C-C chains in the Bmmb phase are conducting and do not undergo any Peierls-like dimerization. Also, it is interesting to note that there is a resemblance between our proposed Li_2C_2 Bmmb structure and Li_xB ($x = 0.90$ and 0.95) [22]. In the latter, each boron attracts one electron from Li (thus becoming isoelectronic to carbon), and B-B chains are formed, engaged in a subnetwork of sixfold Li_6 octahedra. However, in Li_xB the bonding picture is very similar to that calculated for the hypothetical carbon chains (α -carbyne or β -carbyne), which is still intrinsically different from the current case of Li_2C_2 .

The metallic character of compressed Bmmb-type Li_2C_2 is maintained until the

occurrence of the second pressure-induced transition at 215 GPa, when the cubic I2₁3 phase is stabilized. This new phase is insulating with a gap of 2.7 eV [Fig. 2(c)]. Although the carbon atoms in this structure are threefold coordinated, the structure is stabilized by the presence of near tetrahedral sp^3 -hybridized electronic states. For the sp^3 -like hybrids in this case, there are three covalent σ -character bonds connecting each carbon atom to its three nearest neighbors; the remaining two electrons form a lone-pair orbital, which does not participate in the direct bonding with other atoms. The occupied states consist of two distinct groups very similar to those of cg-N [15]. The lowest energy states (more than -6 eV below the top of the valence band) corresponds to the σ C-C bonding states. The second lowest group, ranging from -6 eV to the top of valence band, consists of nonbonding states, which relate to the lone-pair orbital. Although the C-C bond angle (110°) is very close to that in diamond (109°) the bonding scheme is very different, as discussed in Ref. [15].

In summary, our extensive computational study demonstrates that metallic linear chains of carbon can be formed by compressing lithium carbide at relatively low pressure. The conducting properties of these polyynes-like structures embedded in lithium cages originates from the formation of partially filled lone-pair orbitals which favours ionic C-Li bonds and suppresses the tendency towards a Peierls-like insulating behaviour. One important observation of the present study is that the chain-like structure is stable in a pressure range 5-215 GPa—accessible to standardly used high-pressure equipments, therefore we believe that our findings will encourage immediate experimental investigations.

Acknowledgement The authors thanks R. Podloucky for his many helpful suggestions and critical reading. Research at Oak Ridge National Laboratory was sponsored by the Division of Materials Sciences and Engineering, U. S. Department of Energy under contract with UT-Battelle, LLC. This research used resources of the National Energy Research Computing Center, which is supported by the Office of Science of the US Department of Energy. Research at the University of Vienna was supported within the University Focus Research Area *Materials Science* (project “Multi-scale Simulations of Materials Properties and Processes in Materials”).

- [1] A. H. Castro Neto, F. Guinea, N. M. R. Peres, K. S. Novoselov and A. K. Geim *Rev. Mod. Phys.* **2009**, 81, 109-162.
- [2] R. H. Baughman, *Science* **2006**, 312, 1009-1110.
- [3] A. Sun, J. W. Lauher, N. S. Goroff, *Science* **2006**, 312, 1030-1034.
- [4] W. A. Chalifoux, R. McDonald, M. J. Ferguson, and R. R. Tykwinski, *Angew. Chem. Int. Ed.* **2009**, 48, 7915-7919.
- [5] C. Jin, H. Lan, L. Peng, K. Suenaga, and Sumio Iijima, *Phys. Rev. Lett* **2009**, 102, 205501.
- [6] L. Ravagnan, N. Manini, E. Cincuenta, G. Onida, D. Sangalli, C. Motta, M. Devetta, A. Bordoni, P. Piseri, and P. Milani, *Phys. Rev. Lett* **2009**, 102, 245502.
- [7] *Polyynes: Synthesis, Properties and Applications*. F. Cataldo, CRC Press, **2006**.
- [8] H. Shirakawa, *Rev. Mod. Phys.* **2001**, 73, 713-718.
- [9] C. K. Chiang, C. R. Fincher, Jr., Y. W. Park, A. J. Heeger, H. Shirakawa, E. J. Louis, S. C. Gau,

- and Alan G. MacDiarmid, Phys. Rev. Lett **1977**, 39, 1098-1101.
- [10] *One-Dimensional Metals* S. Roth, D. Carroll, Wiley-VCH, **2003**.
- [11] J. Sangster, J. of phase equilibrium and diffusion **2007**, 28, 561-570.
- [12] J. R. Dahn, Phys. Rev. B **1991**, 44, 9170-9177.
- [13] R. Juza, V. Wehle, and H. U. Schuster, Z. Anorg. Allg. Chem. **1967**, 352, 252-257.
- [14] U. Ruschewitz and R. Pöttgen, Z. Anorg. Allg. Chem. **1999**, 625, 1599-1603.
- [15] X.-Q. Chen, C. L. Fu, and R. Podloucky, Phys. Rev. B **2008**, 77, 064103.
- [16] N. Mounet and N. Marzari Phys. Rev. B **2005**, 71, 205214.
- [17] R.W. Lynch and H.G. Drickamer, J. Chem. Phys., **1966**, 44 , 181.
- [18] M. Hanfland, H. Beister, and K. Syassen, Phys. Rev. B **1989**, 39, 12598.
- [19] J. Evers, G. Oehlinger, and A. Weiss, Zeitschrift für Naturforschung, Teil B: Anorganische Chemie, Organische Chemie, **1977**, 32, 1352-1353.
- [20] L. Mitáš and R. M. Martin, Phys. Rev. Lett. **1994**, 72, 2438-2441.
- [21] M. I. Eremets, A. G. Gavriluk, I. A. Trojan, D. A. Dzivenko, and R. Boehler, Nat. Mater. **2004**, 3, 558-563.
- [22] M. Wörle and R. Nesper, Angew Chem Int Ed, **2004** 39, 2349-2353.
- [23] G. Kresse and J. Furthmüller, Comput. Mater. Sci. **1996**, 6, 15-50.
- [24] G. Kresse and D. Joubert, Phys. Rev. B **1999**, 59, 1758-1775.
- [25] P. E. Blöchl, Phys. Rev. B **1994**, 50, 17953-17979.
- [26] J. Perdew, K. Burke, and M. Ernzerhof, Phys. Rev. Lett. **1996**, 77, 3865-3868.
- [27] P. Giannozzi, S. Baroni, N. Bonini, M. Calandra, R. Car, C. Cavazzoni, D. Ceresoli, G. L. Chiarotti, M. Cococcioni, I. Dabo, A. D. Corso, S. d. Gironcoli, S. Fabris, G. Fratesi, R. Gebauer, U. Gerstmann, C. Gougoussis, A. Kokalj, M. Lazzeri, L. Martin-Samos, N. Marzari, F. Mauri, R. Mazzarello, S. Paolini, A. Pasquarello, L. Paulatto, C. Sbraccia, S. Scandolo, G. Sclauzero, A. P. Seitsonen, A. Smogunov, P. Umari, and R. M. Wentzcovitch, J. Phys.: Condens. Matter **2009**, 21, 395502-19.
- [28] C. J. Pickard and R. J. Need, Phys. Rev. Lett. **2006**, 97, 045504.
- [29] A. R. Oganov and C. Glass, J. Chem. Phys. **2006**, 124, 244704
- [30] A. R. Oganov, J. Chen, C. Gatti, Y. Ma, Y. Ma, C. W. Glass, Z. Liu, T. Yu, O. O. Kurakevych, V. L. Solozhenko, Nature **2009**, 457, 863.
- [31] C. Zheng and R. Hoffmann, Inorg. Chem. **1989**, 28, 1074-1080.
- [32] G. Brauer, and A. Mitius, Z. Anorg. Allg. Chem. **1942**, 249, 325-339
- [33] K. Janzon, H. Schäfer, and A. Weiss, Angew. Chem. Int. Ed. **1965**, 4, 245.
- [34] P. Schobinger-Papamantellos, D. B. de Mooij, and K. H. J. Buschow, J. All. Comp. **1992**, 183, 181-186.